Mausam, (1988), **39**, 3, 241-248

551.526.6 : 551.465.73 (267)

Seasonal heat budget estimates of the upper layers in the central Arabian Sea

R. R. RAO*

NOAA/AOML/PhOD

4301 *Rickenbacker, Causeway, Miami, Florida* 33149

(*Received 19 February 1987*)

सार — सभी उपलब्ध ऐतिहासिक बी टी/एक्स बी टी/नेनसेन संचित आंकड़ा सेटों की सहायता से मध्य अरब सागर (मार्सडेन स्कावायर संख्या 066) के सर्वोच्च 200 मी. जलस्तम्भ की ऊष्मीय संरचना में प्रेक्षित ऋतुनिष्ठ परिवर्तनशीलता को प्रस्तुत किया गया है। हैसनरथ और लैम्ब (1979) से उद्धृत धरातल की निवर्त ऊष्मा वृद्धि और उत्तरोत्तर माध्य मासिक उच्चांधर तापमान प्रोफाइल से व्युत्पन्न ताप संग्रहण दर और अवशिष्ट पद के रूप में व्युत्पन्न ऊष्मा के अवसरण के परिप्रेक्ष्य में जल स्तम्भ के ताप बजट आकलनों का विवेचन किया गया है। उपरिस्तर के ताप बजट की प्रेक्षित मौसमी परिवर्तनशीलता पर प्रत्यावर्तित होने वाले मानसून के प्रभाव पर प्रकाश डाला गया है।

ABSTRACT. The observed seasonal variability in the thermal structure of the topmost 200 m water column of the central Arabian Sea (Marsden Square No. 066) is presented with the aid of all the available historic BT/XBT/Nansen cast data sets. The heat budget estimates of the water column are discussed in terms of net surface heat gain extracted from Hastenrath and Lamb (1979) and of heat storage rate derived from successive mean monthly vertical temperature profiles and divergence of heat derived as a residual term. The influence of seasonal reversing monsoons on the observed seasonal variability of heat budget of the upper layers is highlighted.

1. Introduction

The seasonal scale variability in the thermal structure of the upper layers (surface mixed layer and upper thermocline) of the Arabian Sea is mostly governed by the forcing of seasonal reversing monsoons. The sea surface temperature (SST) exhibits bimodality due to heating and cooling regimes caused by the summer and winter monsoons superimposed by the latitudinal march of solar heating. The annual range of SST is highest in the western Arabian Sea and decreases eastward. The SST is known to be controlled by a variety of surface meteorological and sub-surface oceanic processes. Surface heat budget components such as solar radiation, net longwave radiation, sensible and latent heat fluxes, coastal and mid-oceanic upwelling, advection of warm or cold waters, lateral diffusion, entrainment of colder waters from below and the thickness of the mixed layer are all known to contribute to the variability of the SST. The relative importance of these processes vary both in time and space.

Several authors have attempted to explain the interaction between the monsoons and the Arabian Sea both in the temporal and spatial domains. Surface heating during summer (March-May) and cooling during the following monsoon season (June-August), as the dominant signal in the bimodal distribution of SST, has attracted the attention of several workers. Wyrtki (1970) found that over most of the Indian Ocean the yearly cycle of thermal regime is the strongest seasonal signal and is usually far larger than the non-seasonal random fluctuations. Colborn's (1975) results indicate that the monsoon-controlled northern Indian Ocean exhibits thermal structure variations in the upper 500 m that are unique to these latitudes in the oceans of the world. Tunnel (1963) suggested that the advection of cold upwelled waters from the coastal regions is the primary cooling mechanism in the north central Arabian Sea. But Colon (1964) found that the primary process causing the mid-summer cooling in the central Arabian Sea is the change in net surface heat exchange brought in by increased evaporation and decreased incident solar radiation. Wooster *et al.* (1967) found the intensity of cooling increases from May through August along the Somalia and Arabia coasts due to coastal upwelling. Duing and Leetmaa (1980) in their preliminary study of the heat budget of the near surface layers of the Arabian Sea found that in the summer months heat loss due to upwelling more than offset the net heat gain from the atmosphere and that the effect of advection was relatively small. They suggested that the relative importance of these terms will vary from one part of the Arabian Sea to another. Results of McPhaden's (1982) heat budget analysis at a station in the central equatorial Indian Ocean indicated that about 80% of the observed variance in the mixed-layer temperature on monthly time scales can be accounted for by surface heat fluxes. Shetye (1986) pointed out the relative importance of both lateral and vertical advective transports of heat against the surface heat fluxes along 10°N during the

*Permanent affiliation : Naval Physical & Oceanographic Laboratory, Cochin.

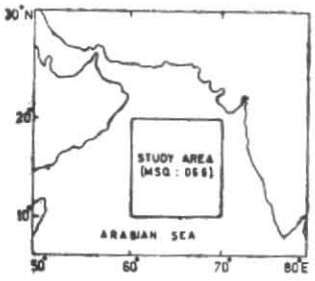

Fig. 1. Study area (Marsden Square No. 066)

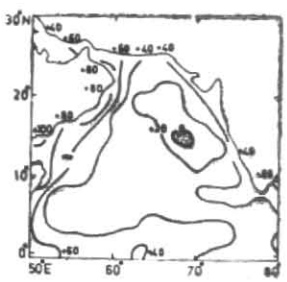

Fig. 2. Net annual oceanic heat gain (W/m²) (*From* Hastenrath and Lamb 1979)

TABLE 1

Month	No. of BT casts	No. of hydrocasts	Total
January	103	8	111
February	30	20	50
March	46	21	67
April	22	20	42
May	27	52	79
June	57	40	97
July	6	15	21
August	16	41	57
September	20	6	26
October	26	28	54
November	28	30	58
December	151	7	158
Total	532	288	820

summer monsoon season. Molinari *et al.* (1986) also resolved the relative importance of surface fluxes, entrainment, lateral advection and vertical diffusion in maintaining the observed seasonal temperature cycle at selected areas in the western Indian Ocean. The prevailing clockwise/anticlockwise surface wind stress curl during summer/winter monsoons produce a dynamic effect resulting in the convergence/divergence of Ekman transports leading to the vertical displacement of isotherms in the thermocline. The seasonal variability in the thermocline, therefore, mostly reflects the relative importance of vertical advective processes. In addition, geostrophic flow in association with the prevailing energetic eddy field (Duing 1971) would also contribute to the observed seasonal variability. The relative contributions of surface heat-exchange processes and lateral and vertical advection to the seasonal heat storage rate are not known in clear terms. An attempt is made to parameterize these processes for the central Arabian Sea where the seasonal summer monsoonal mixed layer deepening is largest and spatial variability in the annual net surface heat gain field is relatively weak (Fig. 1, Marsden Square No. 066) with the available data sets.

2. Data

All the available Nansen cast and BT data from NODC files pertaining to the Marsden Square No. 066 (ten degree square bounded by 10°N-20°N and 60°E-70°E) in the central Arabian Sea are utilized to construct the monthly mean vertical profiles of temperature. Nansen cast temperature data are interpolated at every 5 m interval from the values reported at standard depths for the top 200 m water column following Borkowski and Goulet (1971). Appropriate weights for water-bottle temperature data and BT data are given based on the total number of each type while merging the two sets. The distribution of the data utilized is shown in Table 1. Surface heat budget estimates are extracted for the 10-degree square from Hastenrath and Lamb (1979). Values are read at 2.5° grid and are then averaged out for the 10-degree square for each month. Bunker (1972) provided the long-term mean (25-year averages) values of the surface marine meteorological elements for all the twelve months for this 10-degree square.

3. Methodology

Following Etter (1983) the thermal energy budget of an oceanic water column may be expressed as :

$$Q_S = Q_B + Q_V \qquad (1)$$

where,

Q_S = oceanic heat storage rate (W/m²).

Q_B = net surface heat exchange through short and long wave radiative and turbulent heat exchange processes (W/m²).

Q_V = divergence of heat flux due to lateral and vertical advective processes (W/m²).

The net heat gain term at the sea surface (Q_B) is extracted from Hastenrath and Lamb (1979). The heat storage rate term (Q_S) is derived from successive profiles of mean monthly vertical temperature. Q_S may be expressed as :

$$Q_S = \int_{-D}^{0} \rho\, c_p\, \frac{\partial T_w}{\partial t}\, dz = \frac{\partial H}{\partial t} \qquad (2)$$

where,

T_w = water temperature at depth z

t = time (month)

z = vertical coordinate (positive downward)

c_p = specific heat of seawater at constant pressure

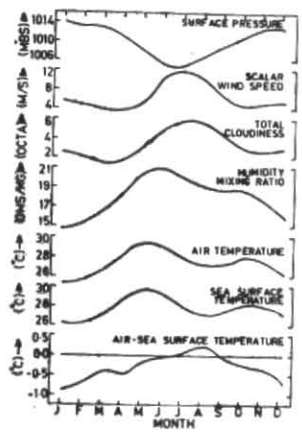

Fig. 3. Annual march of monthly mean surface meteorological elements

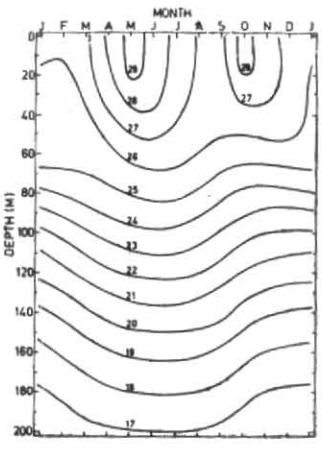

Fig. 4. Annual variation of temperature in the topmost 200 m water column

ρ = density of seawater

D = depth of integration (200 m)

H = heat content of the water column

$$H = \rho\, c_p \int_{-D}^{0} T_w\, dz \qquad (3)$$

Following Emery (1976) the divergence Q_V term may be expressed as :

$$Q_V = V_h \cdot \nabla_h H - \frac{W_D}{D}\,(H - \rho\, c_p\, D\, T_{wD}) \qquad (4)$$

where,

V_h = average horizontal component of velocity in the water column bounded by the surface and depth D

W_D = vertical velocity evaluated at depth D

T_{wD} = water temperature at depth D

Applying the conservation of heat at depth D under some assumptions, Emery (1976) formulated :

$$W_D = \frac{\partial T_w/\partial t}{\overline{\partial T_w/\partial z}} \qquad (5)$$

where, $\frac{\partial T_w}{\partial t}$ = monthly temperature change at D

$\overline{\frac{\partial T_w}{\partial z}}$ = mean monthly vertical temperature gradient at D

4. Analysis and discussion

All the available marine meteorological data for MSQ 066 collected during 1948-1972 have been compiled by Bunker (1972). These values are utilized to describe the near surface climatic conditions as some of the near surface climatic elements described here are not given on monthly resolution by Hastenrath and Lamb (1979). The distributions of monthly means of these meteorological elements are shown in Fig. 3. The influence of both the monsoons is distinctly seen in all the meteorological elements. The surface pressure varies between 1006 and 1014 mb with the occurrence of highest and lowest values during winter and summer monsoon seasons respectively. The scalar wind speed ranges between 4 and 12 m/s with the highest values occurring during the summer monsoon season. Visually observed cloudiness ranges between 2 & 6 octas with the peak values appearing during the summer monsoon season. Humidity mixing ratio of the air progressively increases from 15 to 21g/kg from January to May/June and decreases thereafter. Both air and sea surface temperatures show bimodal distributions with an approximate annual range of 4°C. Pre-monsoonal heating from March to May followed by summer monsoonal cooling are apparent in the temperature distributions of air and surface water. The same cycle is repeated with a mild warming phase from August to October and with a mild cooling phase from October to January. The air-sea temperature differences are weak (<1° C) throughout the year, thus indicating neutral equilibrium conditions near the surface.

Hastenrath and Lamb (1979) estimated net oceanic heat gain for the Indian Ocean with the data base of 60 years. Fig. 2 shows the distribution of net annual oceanic heat gain for the Arabian Sea extracted from Hastenrath and Lamb (1979). Positive values imply heat gain to the ocean. The distribution shows net heat gain by the ocean on an annual cycle. The values are relatively higher in the coastal regions with strong lateral gradients towards the open ocean. This annual accumulation of heat at the surface necessitates the redistribution of the same through other oceanic processes as advection and diffusion both downward and southward. However, these heat gain estimates are to be viewed under the following constraints : (i) the collection of surface marine meteorological data are mostly biased to both concentrated shipping lanes and fair weather conditions as these ships tend to avoid rough weather conditions and/or areas ; (ii) the authors have used constant values for the exchange coefficients in the estimation of turbulent heat exchange terms. These exchange coefficients are known to depend on the near surface wind strength and atmospheric stability regimes. During the disturbed weather conditions the numerical values of these exhange coefficients are not expected to remain constant. Both these reasons probably contribute to the over-estimation of net oceanic heat gain distribution shown in Fig. 2.

The merged data set of vertical temperature profiles are smoothed in the temporal domain passing the data through the Han window. Depth-time section of temperature for the top 200 m water column (Fig. 4) is constructed through linear interpolation. The topmost 50 m layer or so exhibits a well defined bimodal nature with alternating heating and cooling regimes but with unequal magnitudes. The downward penetration of

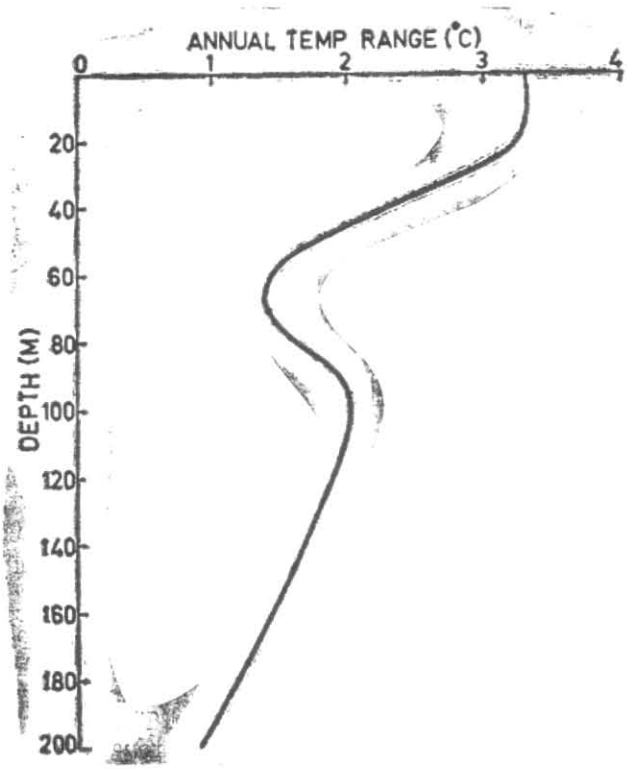

Fig. 5. Annual range of temperature in the topmost 200 m water column

these regimes also differed. Pre-monsoonal heating and summer monsoonal cooling of about 3°C and post-monsoonal heating and winter cooling of about 2°C is conspicuously noticed in the top 40-50 m layer. Below 60 m depth, isotherms are parallel with a concave shape in the themocline. Isotherms are displaced downward during the summer monsoon season and upward during the other part of the layer. The topography of these isotherms suggest the dynamic response on a basin scale due to the Ekman type of convergence/divergence caused by the prevailing clockwise/anticlockwise surface wind stress curl during the summer/winter monsoon seasons. The amplitude of the isotherm displacement is about 25 m implying an upwelling/sinking rate of 2 m/month in the upper thermocline. Large-scale wind stress curl is well known to influence the topography of the isotherms below the mixed layer through an Ekman type of pumping (Yoshida and Mao 1957). Meyers (1979) reported a good agreement between Ekman forcing and thermocline displacements in the region 10°-15°N of the Pacific Ocean. The vertical thermal gradient in the thermocline moderately decreased with depth. These vertical advective processes are, therefore, expected to play an important role in the observed seasonal temperature changes in the upper thermocline.

The annual range of temperature in the top 200 m water column is shown in Fig. 5. The range is highest in the top 20 m layer (>3°C). This large value is resulted due to the strong heating and cooling cycles caused by the monsoons under variable seasonal solar heating. Below this layer the range progressively decreased downward, reaching a minimum value around 70 m depth. This level approximately coincides with the annual maximum of the mixed layer depth for this area. A mild increase in the range is evident in the 70-100 m layer. The secondary maximum occurred around 100 m depth followed by a gradual reduction downward. This maximum around 100 m depth might have been due to large amplitude of the isotherm displacement caused by the dynamic response of the ocean to the reversing monsoonal wind stress curl. The strong vertical thermal gradient also influences the observed large amplitude of the vertical oscillation.

The mixed layer depth (MLD) is estimated from the mean vertical temperature profile as the depth where the temperature is less by 1° C from SST. The annual march of MLD and SST are shown in Fig. 6. Both the the curves show bimodal nature. The broad agreement in their phase indicates that the observed variability in MLD and SST has probably resulted from the same causative factors. The mixed layer shoaling is generally caused by net surface oceanic heat gain, leading to near surface thermal stratification, upwelling/divergence, internal/inertial waves, while deepening is attributed to wind and wave mixing, convective turnover caused by buoyancy flux, dynamic instability below the layer/stratification and convergence. The MLD varied between

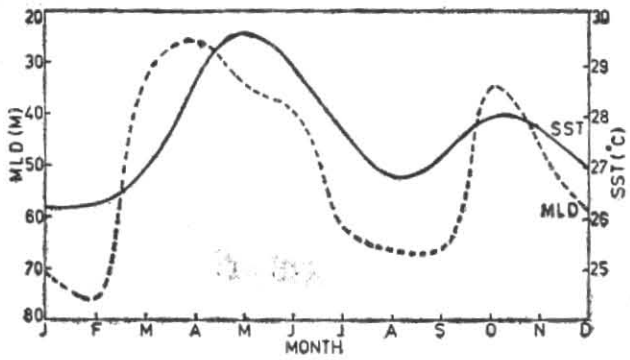

Fig. 6. Annual march of SST and MLD

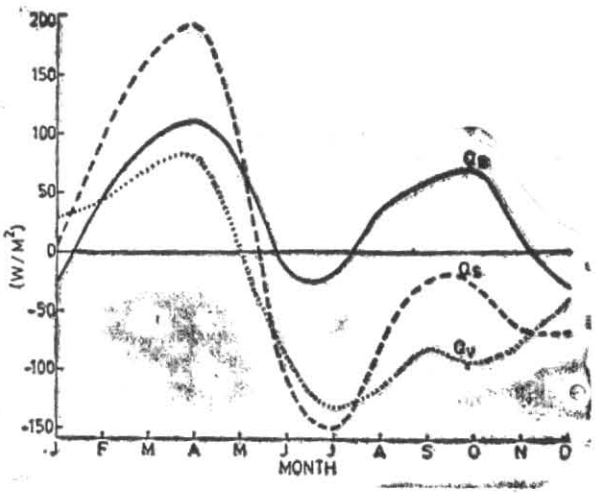

Fig. 7. Annual march of net oceanic heat gain (Q_B), heat storage rate (Q_S) and heat advection (Q_V) in W/m²

25 and 75 m with the occurrence of minima in April and October and maxima in February and September. Steep shoaling resulted during the pre-monsoon season due to intense solar heating of about 3°C when the turbulent heat losses were very weak across the air-sea interface. A progressive deepening of 40 m from April to September resulted due to the enhanced mixing caused by the summer monsoonal forcing with an associated surface cooling of nearly 3° C. During this period the deepening rate is highest when the strength of the summer monsoon is at its peak. Withdrawal of the summer monsoon and resulting clear skies lead to a secondary warming of about 1.5°C from August to October. During the following winter monsoon season the layer cooling and deepening are of the order of 2°C and 40 m respectively. These observed seasonal cycles clearly reveal the importance of the forcings of the reversing monsoons in regulating the variability of SST and MLD.

The annual march of net surface heat gain (Q_B), heat storage (Q_S), and heat advection (Q_V) as the residual term for the top 200 m water column is shown in Fig. 7. Positive values indicate heat gain to the ocean. The relative contributions of Q_B and Q_V to the observed variability of Q_S is evident from this figure. Over an annual cycle Q_B mostly contributed to the supply of heat with minor exceptions during June-July (summer monsoon season) and December-January (winter monsoon season). A steep rise in the heat storage rate during the first four months suggests accumulation of heat mostly through solar heating and advective processes during this period. The heat storage rate begins to recede in a dramatic way during May, June and July under the influence of the summer monsoonal forcing. This rapid reduction in Q_S seems to be mostly determined by Q_V if the estimates of Q_B are reasonably accurate. This heat drainage through advection persists from May through December to compensate for the anomalous accumulation of heat through Q_B. Interestingly, all the three curves are in phase although their magnitudes differed. The annual march of the integrals of these estimates (Fig. 8) show some interesting features. The integral of all the three terms monotonically increased from January to May. Although ΣQ_B shows further increase during the rest of the year, ΣQ_S registers a gradual decrease from May and reaches zero by December, thus, indicating a balance on an annual cycle. The reduction in ΣQ_S from May is controlled by ΣQ_V suggesting drainage of heat during April/May to December. There is an exact balance between the annual integrals of ΣQ_B and ΣQ_V ($\sim$400 W/m²).

In order to understand the relative contributions of horizontal and vertical transports of heat, the advection term (Q_V) is further resolved into lateral (in the top 200 m) (Q_{VH}) and vertical at 200 m depth (Q_{VW}) contributions with the aid of Eqn. (4) and the distributions are shown in Fig. 9. The vertical heat transport at 200 m depth shows three typical regimes : downward transport of warmer waters from January to May, very weak transports from May to August, and upward transport of colder water from August to December. The magnitudes of the slopes of the isotherms (Fig. 4) are reflected in the estimates of Q_{VW}. On the other hand, Q_{VH} is mostly negative (with the only exception in April) implying divergence of accumulated heat in the top 200 m water column. During the summer season Q_{VH} is found to be larger than Q_{VW}.

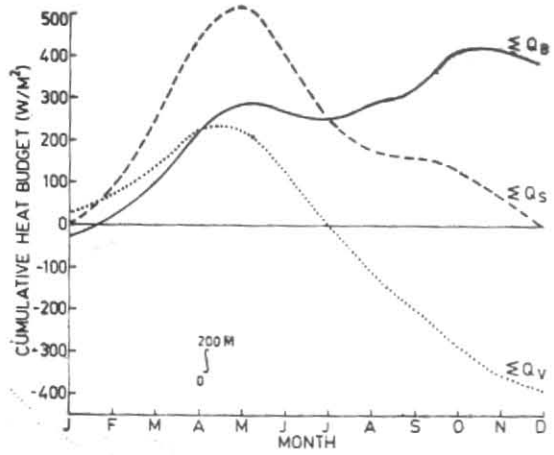

Fig. 8. Annual march of cumulative net oceanic heat gain (ΣQ_B), heat storage rate (ΣQ_S) and heat advection (ΣQ_V) in W/m²

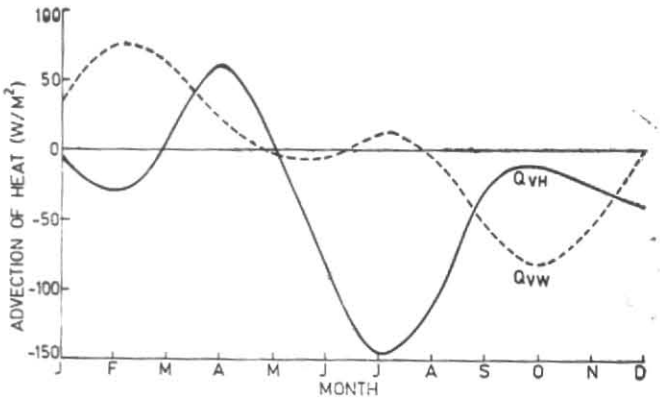

Fig. 9. Annual march of lateral (Q_{VH}) and vertical (Q_{VW}) heat advection in W/m²

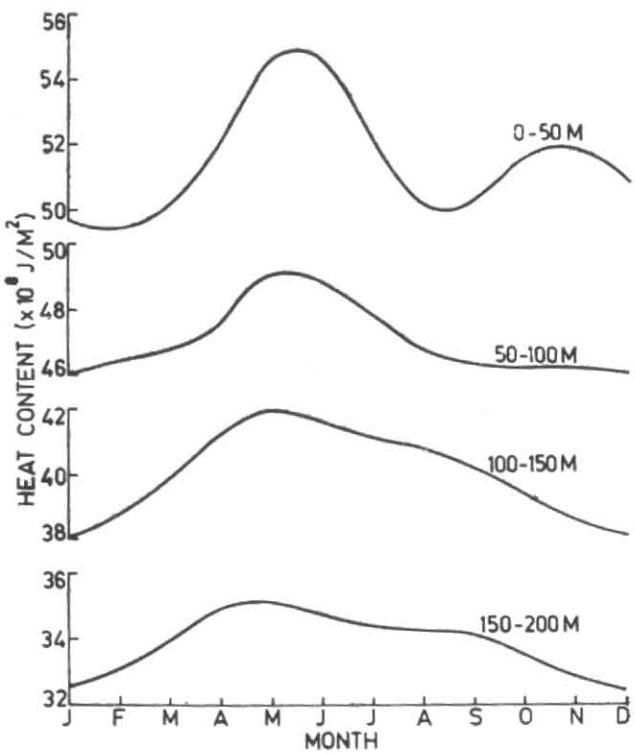

Fig. 10. Annual march of heat content in different layers (J/m²)

In the following section an attempt is made to break down these budget estimates for each 50 m slab from surface to 200 m depth. The annual variability of the heat content in each 50 m slab is shown in Fig. 10. As expected, the heat content of the slabs decreased with depth. A bimodal distribution is evident only in the topmost 50 m layer while a unimodal distribution is noticed in the other three slabs between 50 and 200 m depths. The impact of the winter monsoon in the central Arabian Sea appears to be limited to 50 m or so. Accumulation of heat from

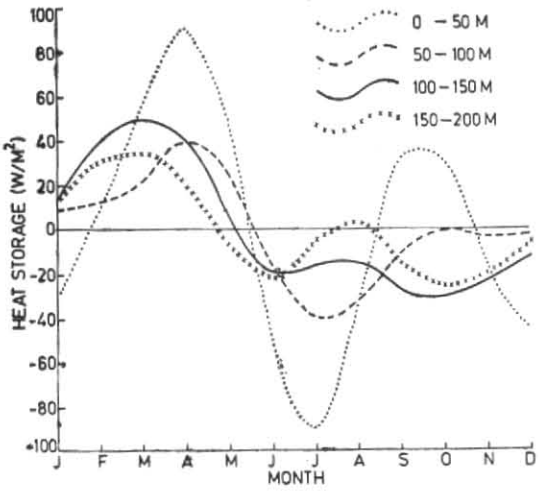

Fig. 11. Annual march of heat storage rate in different layers (W/m²)

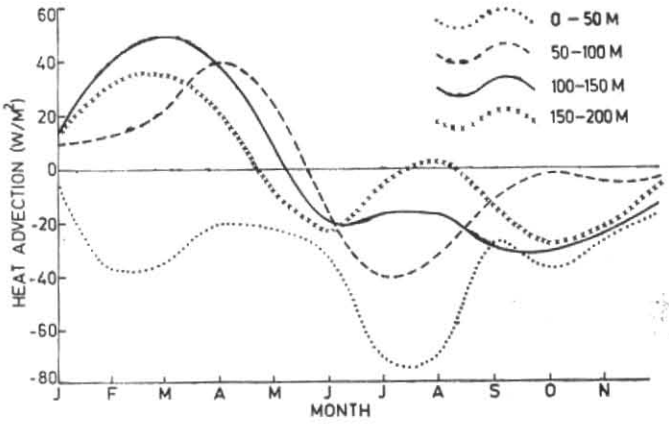

Fig. 12. Annual march of heat advection in different layers (W/m²)

January to May is a common feature in all the four slabs. The accumulation is rapid while the depletion is rather slow. The amplitude of the annual oscillation decreased with depth. The variability of the heat storage rates in all the four slabs is shown in Fig. 11. The magnitude and amplitude of Q_S for the topmost 50 m slab is significantly different from those of other three. Large seasonal variations are confined only to the topmost 50 m layer under the influence of surface heat exchanges and advection associated with the reversing monsoonal forcings. An agreement in phase in the upper two slabs is also evident. The heat storage rates in the lower two slabs resemble each other.

The heat advection term (Q_V) for the top 200 m water column is decomposed for each 50 m slab and the derived annual variability is shown in Fig. 12. Positive values imply convergence of heat in the water column. In the topmost 50 m layer heat diverged throughout the year with its peak value occurring during July-August. This heat divergence might have been accomplished either due to export of warm waters during the winter monsoon season and/or due to the import of cold waters during the summer monsoon season. The colder waters upwelled off the Somalia and Arabia coasts appear to have advected into the study area during July-August. The corresponding pattern for the deeper slabs is dissimilar to that of the topmost 50 m slab. In the deeper slabs accumulation of heat is noticed from January to May while depletion is seen during the rest of the year in accordance with the vertical displacement of isotherms in the upper thermocline.

5. Summary and conclusions

All the surface marine meteorological elements show strong seasonal cycles. The net surface heat gain estimated by Hastenrath and Lamb (1979) suggest accumulation of heat in the Arabian Sea on an annual cycle. Heat divergence through lateral and vertical advection and diffusion (not estimated in this study) must become important to maintain thermal equilibrium on an annual mode. The semi-annual signal noticed in the surface temperature appears to have penetrated only to a depths of 40 to 50 m under the heating and cooling regimes through the course of one year. Below 60 m depth, annual signal is noticed in the vertical displacement of isotherms in the thermocline. The topography of the isotherms might have manifested as a result of Ekman type of divergence caused by the prevailing surface wind stress curl. The surface mixed layer depth exhibited a similar variation as that of SST suggesting that both these variables are influenced by the same causative factors. The heat storage rate is positive (accumulation of heat) during January through May and with the onset and sway of the summer monsoon this accumulated heat is drained out in a dramatic way during May, June and July. Relatively large seasonal variations are confined to the topmost 50 m water column compared to deeper slabs of water. Heat appears to have diverged out of the topmost 50 m water column throughout the year while in the deeper slabs accumulation of heat is noticed from January to May and depletion of heat is found during the rest of the year.

References

Borkowski, M.R. and Goulet, J.R., 1971, Comparison of methods for interpolating oceanographic data, *Deep-Sea Res.*, **18**, 269-274.

Colborn, J.G., 1975, The thermal structure of the Indian Ocean, IIOE Oceanographic Monographs No. 2. The Univ. Press of Hawaii, Honolulu.

Colon, J.A., 1964, On interactions between the southwest monsoon current and the sea surface over the Arabian Sea, *Indian J. Met. Geophys.*, **15**, 2, pp. 183-200.

Duing, W., 1971, The structure of sea surface temperatures in monsoonal areas, *Studies in Physical Oceanography*, Vol. I, A tribute to George Wust on his 80th birthday, 1-17.

Duing, W. and Leetmaa, A., 1980, Arabian Sea cooling : A preliminary heat budget, *J. Phys. Oceanogr.*, **10**, 302-312.

Emery, W.J., 1976, The role of vertical motion in the heat budget of the upper northeastern Pacific Ocean, *J. Phys. Oceanogr.*, **6**, 299-305.

Etter, P.C., 1983, Heat and freshwater budgets of the Gulf of Mexico, *J. Phys. Oceanogr.*, **13**, 2058-2069.

Hastenrath, S. and Lamb, P.J., 1979, *Climatic Atlas of the Indian Ocean* (Parts I and II), Univ. of Wisconsin Press, Madison WI.

McPhaden, M.J., 1982, Variability in the central equatorial Indian Ocean, Part II : Oceanic heat and turbulent energy balances, *J. Mar. Res.*, **40**, 2, 403-419.

Meyers, G., 1979, Annual variation in the slope of the 14°C isotherm along the equator in the Pacific, *J. Phys. Oceanogr.*, **9**, 885-891.

Molinari, R.L., Swallow, J. and Festa, J., 1986, Evolution of the near-surface thermal structure in the western Indian Ocean during FGGE, 1979, *J. Mar. Res.*, **44**, 739-762.

Shetye, S.R., 1986, A model study of the seasonal cycle of the Arabian Sea surface temperature, *J. Mar. Res.*, **44**, 521-542.

Tunnel, G.A., 1963, Sea temperature fluctuations in the Red Sea, the Gulf of Aden and the Arabian Sea, *Mar. Obsrv.*, **33**, 192-201.

Wooster, W.S., Scheefer, M.B. and Robinson, M.K., 1967, *Atlas of the Arabian Sea for Fishery Oceanography*, IMR Reference, 67-12, Univ. of California, La Jolla, California, USA.

Wyrtki, K., 1970, *Oceanographic Atlas of the International Indian Ocean Expedition*, National Science Foundation, NSF-IOE-1, Washington, D.C.

Yoshida, K. and Mao, H.L., 1957, A theory of upwelling of large horizontal extent, *J. Mar. Res.*, **16**, 1, 40-54.